

Photocytotoxic 3d-Metal Scorpionates with a 1,8-Naphthalimide Chromophore Showing Photoinduced DNA and Protein Cleavage Activity

Sovan Roy,[†] Sounik Saha,[†] Ritankar Majumdar,[‡] Rajan R. Dighe,[‡] and Akhil R. Chakravarty^{*,†}

[†]Department of Inorganic and Physical Chemistry and [‡]Department of Molecular Reproduction, Development and Genetics and Indian Institute of Science, Bangalore 560012, India

Received April 15, 2009

Ternary 3d-metal complexes of formulation $[M(\text{Tp}^{\text{Ph}})(\text{py-nap})](\text{ClO}_4)$ (**1–3**), where M is Co(II) (**1**), Cu(II) (**2**), and Zn(II) (**3**); Tp^{Ph} is anionic tris(3-phenylpyrazolyl)borate; and py-nap is a pyridyl ligand with a conjugated 1,8-naphthalimide moiety, have been prepared from the reaction of metal perchlorate with KTp^{Ph} and py-nap in CH_2Cl_2 . The complexes have been characterized from analytical and physicochemical data. The complexes are stable in solution as evidenced from the electrospray ionization mass spectrometry data. The complexes show good binding propensity with calf thymus (CT) DNA, giving binding constant (K_b) values of $\sim 10^5 \text{ M}^{-1}$ and a molecular “light-switch” effect that results in an enhancement of the emission intensity of the naphthalimide chromophore on binding to CT DNA. The complexes do not show any hydrolytic cleavage of DNA. They show poor chemical nuclease activity in the presence of 3-mercaptopropionic acid or hydrogen peroxide (H_2O_2). The Co(II) and Cu(II) complexes exhibit oxidative pUC19 DNA cleavage activity in UV-A light of 365 nm. The Zn(II) complex shows moderate DNA photocleavage activity at 365 nm. The Cu(II) complex **2** displays photoinduced DNA cleavage activity in red light of 647.1 nm and 676 nm and near-IR light of $>750 \text{ nm}$. A mechanistic study in UV-A and visible light suggests the involvement of the hydroxyl radical as the reactive species in the DNA photocleavage reactions. The complexes also show good bovine serum albumin (BSA) protein binding propensity, giving K_{BSA} values of $\sim 10^5 \text{ M}^{-1}$. Complexes **1** and **2** display significant photoinduced BSA cleavage activity in UV-A light. The Co(II) complex **1** shows a significant photocytotoxic effect in HeLa cervical cancer cells on exposure to UV-A light of 365 nm, giving an IC_{50} value of $32 \mu\text{M}$. The IC_{50} value for the py-nap ligand alone is $41.42 \mu\text{M}$ in UV-A light. The IC_{50} value is $>200 \mu\text{M}$ in the dark, indicating poor dark toxicity of **1**. The Cu(II) complex **2** exhibits moderate photocytotoxicity and significant dark toxicity, giving IC_{50} values of $18.6 \mu\text{M}$ and $29.7 \mu\text{M}$ in UV-A light and in the dark, respectively.

Introduction

Transition metal complexes that are capable of cleaving DNA and proteins under physiological conditions are of interest in the development of metal-based anticancer agents.^{1–10} Metal complexes with their tunable coordination geometry and

versatile redox and spectral properties provide a wide scope of possibilities in designing systems that are suitable for targeting DNA and proteins to control primary and malignant secondary tumors. For example, iron-bleomycins and related model complexes are known to show chemical nuclease activity cleaving DNA in an oxidative manner.^{10–13} The metal-based chemotherapeutic drugs like cis-platin and its

*To whom correspondence should be addressed. Fax: 91-80-23600683. E-mail: arc@ipc.iisc.ernet.in.

(1) Chifotides, H. T.; Dunbar, K. R. *Acc. Chem. Res.* **2005**, *38*, 146. Angeles-Boza, A. M.; Chifotides, H. T.; Aguirre, J. D.; Chouai, A.; Fu, P. K.-L.; Dunbar, K. R.; Turro, C. *J. Med. Chem.* **2006**, *49*, 6841. Angeles-Boza, A. M.; Bradley, P. M.; Fu, P. K.-L.; Wicke, S. E.; Bacsá, J.; Dunbar, K. R.; Turro, C. *Inorg. Chem.* **2004**, *43*, 8510. Bradley, P. M.; Angeles-Boza, A. M.; Dunbar, K. R.; Turro, C. *Inorg. Chem.* **2004**, *43*, 2450.

(2) Bednarski, P. J.; Mackay, F. S.; Sadler, P. J. *Anticancer Agents Med. Chem.* **2007**, *7*, 75. Dyson, P. J.; Sava, G. *Dalton Trans.* **2006**, 1929.

(3) Rose, M. J.; Fry, N. L.; Marlow, R.; Hinck, L.; Mascharak, P. K. *J. Am. Chem. Soc.* **2008**, *130*, 8834.

(4) Brindell, M.; Kuliš, E.; Elmroth, S. K. C.; Urbańska, K.; Stochel, G. *J. Med. Chem.* **2005**, *48*, 7298.

(5) Heringova, P.; Woods, J.; Mackay, F. S.; Kasparkova, J.; Sadler, P. J.; Brabec, V. *J. Med. Chem.* **2006**, *49*, 7792.

(6) Sigman, D. S.; Mazumder, A.; Perrin, D. M. *Chem. Rev.* **1993**, *93*, 2295. Boerner, L. K. J.; Zaleski, J. M. *Curr. Opin. Chem. Biol.* **2005**, *9*, 135.

(7) Kumar, C. V.; Buranaprapuk, A.; Opiteck, G. J.; Moyer, M. B.; Jockusch, S.; Turro, N. J. *Proc. Natl. Acad. Sci. U. S. A.* **1998**, *95*, 10361. Buranaprapuk, A.; Leach, S. P.; Kumar, C. V.; Bocarsly, J. R. *Biochim. Biophys. Acta* **1998**, *1387*, 309.

(8) Meggers, E. *Chem. Commun.* **2009**, 1001.

(9) Zhu, L.; Kostic, N. M. *J. Am. Chem. Soc.* **1993**, *115*, 4566. Rajendiran, V.; Palaniandavar, M.; Swaminathan, P.; Uma, L. *Inorg. Chem.* **2007**, *46*, 10446. Milović, N. M.; Dutc, L.-M.; Kostic, N. M. *Chem.—Eur. J.* **2003**, *9*, 5097.

(10) Umezawa, H. *Prog. Biochem. Pharmacol.* **1976**, *11*, 18. Burger, R. M. *Chem. Rev.* **1998**, *98*, 1153.

(11) Chen, J.; Stubbe, J. *Nat. Rev. Cancer* **2005**, *5*, 102.

(12) Hertzberg, R. P.; Dervan, P. B. *J. Am. Chem. Soc.* **1982**, *104*, 313. Mukherjee, A.; Dhar, S.; Nethaji, M.; Chakravarty, A. R. *Dalton Trans.* **2005**, 349.

(13) Van den Berg, T. A.; Feringa, B. L.; Roelfes, G. *Chem. Commun.* **2007**, 180.

analogues are known for cytotoxicity, but they suffer from side effects along with drug-resistance problems.^{14–19} Among different modes of oxidative DNA cleavage, photodynamic therapy (PDT) has emerged as a viable alternative mode of treatment of cancer.^{20–24} PDT involves selective activation of the photosensitizing drug at the cancer cells, leading to only a localized photocytotoxic effect, thus leaving the healthy cells unaffected. Organic dyes like porphyrin and phthalocyanine bases have been extensively studied as PDT agents considering their photosensitizing ability within the PDT spectral window of 600–800 nm.^{25–29} Photofrin, the currently used PDT drug, is a hematoporphyrin species that on photoactivation of its lowest energy Q-band at ~630 nm generates a (π - π^*) state with subsequent formation of the triplet state that activates molecular oxygen to cytotoxic singlet oxygen (1O_2) by energy transfer.²⁰ Such organic dyes along with squaraines and boradiazaindacenes generally follow the mechanistic pathway that involves the formation of singlet oxygen (1O_2) as an

important criterion for their anticancer activity.^{25–32} In contrast, transition metal complexes with low-energy d–d or charge transfer band(s) could photocleave DNA following alternate mechanistic pathways like type-I or photoredox processes in the presence of redox active metal ions.^{33–35}

Although various types of organic dyes have been studied as potential PDT agents, the chemistry of metal-based PDT agents is relatively unexplored. A six-coordinate platinum(IV) complex having two photolabile trans-azide ligands has recently been shown to form a cisplatin analogue that shows a photocytotoxic effect.³⁶ Dirhodium(II,II) complexes of phenanthroline bases are reported to show photocytotoxicity in visible light.¹ Ruthenium nitrosyl complexes on photoactivation in visible light are known to generate cytotoxic nitric oxide.³ UV-light-induced photocytotoxicity has been reported for $[RuCl_2(DMSO)_4]$ and transplatin.^{4,5} While these metal-based PDT agents have heavier metal ions, the utility of bioessential 3d transition metal complexes as PDT agents is virtually unknown in the literature. We have recently reported iron(III) and vanadium(IV) complexes having dipyrrophenazine (dppz) showing photocytotoxicity in HeLa cells in visible light.^{37,38} Besides the development of the chemistry of metal-based PDT agents, current efforts are also directed toward designing metal-based antimetastasis agents to control tumor malignancy.² Ruthenium(II) coordination complexes and (η^6 -arene)ruthenium(II) organometallic complexes are known to act as inhibitors to protein kinases that are generally overexpressed in the cancer cells causing secondary tumor formation.^{2,39,40} It is thus of importance to design complexes of bioessential 3d transition metal ions that could show photoinduced DNA and protein cleavage activity in the absence of any external additives for their potential application as PDT and antimetastasis agents.

In designing the complexes of Co(II), Cu(II), and Zn(II), we have chosen a sterically demanding monoanionic tris(3-phenylpyrazolyl)borate (Tp^{Ph}) ligand to form a $\{M(Tp^{Ph})\}$ molecular bowl in a ternary structure $[M(Tp^{Ph})(py-nap)](ClO_4)$ (1–3) that sterically encloses a pyridyl ligand having a 1,8-naphthalimide (py-nap) chromophore. In our earlier reports, we have shown that such ternary complexes of the type $[M(Tp^{Ph})(B)](ClO_4)$, where M is a bivalent 3d metal ion and B is a photoactive phenanthroline base, show poor chemical nuclease activity but significant photoinduced DNA cleavage activity due to the steric bowl of Tp^{Ph} that effectively encloses the $\{M(B)\}$ moiety.^{41–43} The present work stems from our interest in exploring the effect of the

(14) Rosenberg, B.; VamCamp, L.; Trosko, J. E.; Mansour, V. H. *Nature* **1969**, *222*, 385.

(15) Zhang, C. X.; Lippard, S. J. *Curr. Opin. Chem. Biol.* **2003**, *7*, 481. Jung, Y.; Lippard, S. J. *Biochemistry* **2003**, *42*, 2664. Jamieson, E. R.; Lippard, S. J. *Chem. Rev.* **1999**, *99*, 2467.

(16) Galanski, M.; Jakupec, M. A.; Keppler, B. K. *Curr. Med. Chem.* **2005**, *12*, 2075. Kang, H. C.; Kim, I.-J.; Park, H.-W.; Jang, S.-G.; Ahn, S.-A.; Yoon, S. N.; Chang, H. J.; Yoo, B. C.; Park, J.-G. *Cancer Lett.* **2007**, *247*, 40.

(17) Dhar, S.; Liu, Z.; Thomale, J.; Dai, H.; Lippard, S. J. *J. Am. Chem. Soc.* **2008**, *130*, 11467. Dhar, S.; Gu, F. X.; Langer, R.; Farokhzad, O. C.; Lippard, S. J. *Proc. Natl. Acad. Sci. U. S. A.* **2008**, *105*, 17356.

(18) Nishiyama, N.; Kato, Y.; Sugiyama, Y.; Kataoka, K. *Pharm. Res.* **2001**, *18*, 1035. Neuse, E. W.; Mphphu, N.; Netshifhe, H. M.; Johnson, M. T. *Polym. Adv. Technol.* **2002**, *13*, 884.

(19) Stochel, G.; Wanad, A.; Kulis, E.; Stasicka, Z. *Coord. Chem. Rev.* **1998**, *171*, 203.

(20) Bonnett, R. *Chemical Aspects of Photodynamic Therapy*; Gordon & Breach: London, U. K., 2000.

(21) Detty, M. R.; Gibson, S. L.; Wagner, S. J. *J. Med. Chem.* **2004**, *47*, 3897.

(22) Ali, H.; van Lier, J. E. *Chem. Rev.* **1999**, *99*, 2379.

(23) Sternberg, E. D.; Dolphin, D.; Brückner, C. *Tetrahedron* **1998**, *54*, 4151.

(24) Henderson, B. W.; Busch, T. M.; Vaughan, L. A.; Frawley, N. P.; Babich, D.; Sosa, T. A.; Zollo, J. D.; Dee, A. S.; Cooper, M. T.; Bellnier, D. A.; Greco, W. R.; Oseroff, A. R. *Cancer Res.* **2000**, *60*, 525.

(25) Rodriguez, M. E.; Moran, F.; Bonansea, A.; Monetti, M.; Fernandez, D. A.; Strassert, C. A.; Rivarola, V.; Awruch, J.; Dicalio, L. E. *Photochem. Photobiol. Sci.* **2003**, *2*, 988.

(26) Pandey, R. K.; Sumlin, A. B.; Constantine, S.; Aoudia, M.; Potter, W. R.; Bellnier, D. A.; Henderson, B. W.; Rodgers, M. A.; Smith, K. M.; Dougherty, T. J. *Photochem. Photobiol.* **1996**, *64*, 194.

(27) Stranadko, E.; Skobelkin, O.; Litwin, G.; Astrakhankina, T. *Proc. SPIE-Int. Soc. Opt. Eng.* **1994**, *2325*, 240. Richter, A. M.; Kelly, B.; Chow, J.; Liu, D. J.; Towers, G. M. N.; Dolphin, D.; Levy, J. G. *J. Natl. Cancer Inst.* **1987**, *79*, 1327. Levy, J. G.; Chan, A.; Strong, H. A. *Proc. SPIE-Int. Soc. Opt. Eng.* **1996**, *2625*, 86.

(28) Morgan, A. R.; Garbo, G. M.; Keck, R. W.; Selman, S. H. *Cancer Res.* **1988**, *48*, 194. Bonnett, R.; White, R. D.; Winfield, U.-J.; Berenbaum, M. C. *Biochem. J.* **1989**, *261*, 277. Dilkes, M. G.; de Jode, M. L.; Rowntree-Taylor, A. *Lasers Med. Sci.* **1997**, *11*, 23. Razum, N.; Snyder, A.; Dorion, D. *Proc. SPIE-Int. Soc. Opt. Eng.* **1996**, *2675*, 43.

(29) Nelson, J. S.; Roberts, W. G.; Berns, J. M. *Cancer Res.* **1987**, *47*, 4681.

(30) Ramaiah, D.; Eckert, I.; Arun, K. T.; Weidenfeller, L.; Epe, B. *Photochem. Photobiol.* **2004**, *79*, 99.

(31) Atilgan, S.; Ekmecki, Z.; Dogan, A. L.; Guc, D.; Akkaya, E. U. *Chem. Commun.* **2006**, 4398.

(32) Szacilowski, K.; Macyk, W.; Drzewiecka-Matuszek, A.; Brindell, M.; Stochel, G. *Chem. Rev.* **2005**, *105*, 2647.

(33) Lahiri, D.; Bhowmick, T.; Pathak, B.; Shameema, O.; Patra, A. K.; Ramakumar, S.; Chakravarty, A. R. *Inorg. Chem.* **2009**, *48*, 339. Maity, B.; Roy, M.; Chakravarty, A. R. *J. Organomet. Chem.* **2008**, *693*, 1395. Roy, M.; Pathak, B.; Patra, A. K.; Jemmis, E. D.; Nethaji, M.; Chakravarty, A. R. *Inorg. Chem.* **2007**, *46*, 11122. Dhar, S.; Senapati, D.; Reddy, P. A. N.; Das, P. K.; Chakravarty, A. R. *Chem. Commun.* **2003**, 2452.

(34) Maurer, T. D.; Kraft, B. J.; Lato, S. M.; Ellington, A. D.; Zaleski, J. M. *Chem. Commun.* **2000**, 69.

(35) Burrows, C. J.; Muller, J. G. *Chem. Rev.* **1998**, *98*, 1109. Armitage, B. *Chem. Rev.* **1998**, *98*, 1171.

(36) Mackay, F. S.; Woods, J. A.; Heringová, P.; Kašpárková, J.; Pizarro, A. M.; Moggach, S. A.; Parsons, S.; Brabec, V.; Sadler, P. J. *Proc. Natl. Acad. Sci. U. S. A.* **2007**, *104*, 20743.

(37) Saha, S.; Majumdar, R.; Roy, M.; Dighe, R. R.; Chakravarty, A. R. *Inorg. Chem.* **2009**, *48*, 2652.

(38) Sasmal, P. K.; Saha, S.; Majumdar, R.; Dighe, R. R.; Chakravarty, A. R. *Chem. Commun.* **2009**, 1703.

(39) Debreczeni, J. É.; Bullock, A. N.; Atilla, G. E.; Williams, D. S.; Bregman, H.; Knapp, S.; Meggers, E. *Angew. Chem., Int. Ed.* **2006**, *45*, 1580.

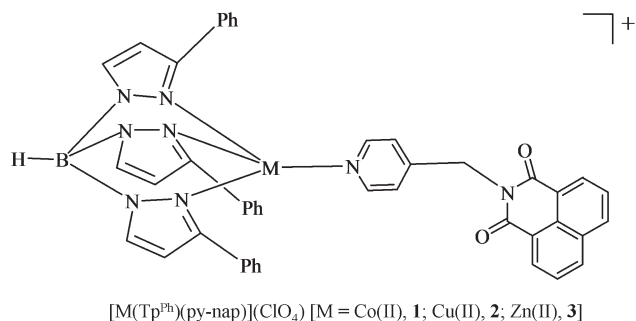
(40) Atilla-Gokcumen, G. E.; Pagano, N.; Streu, C.; Maksimoska, J.; Filippakopoulos, P.; Knapp, S.; Meggers, E. *Chem. Bio. Chem.* **2008**, *9*, 2933.

(41) Dhar, S.; Reddy, P. A. N.; Nethaji, M.; Mahadevan, S.; Saha, M. K.; Chakravarty, A. R. *Inorg. Chem.* **2002**, *41*, 3469.

(42) Dhar, S.; Chakravarty, A. R. *Inorg. Chem.* **2005**, *44*, 2582.

(43) Roy, S.; Patra, A. K.; Dhar, S.; Chakravarty, A. R. *Inorg. Chem.* **2008**, *47*, 5625.

Chart 1. Ternary Complexes $[M(\text{Tp}^{\text{Ph}})(\text{py-nap})](\text{ClO}_4)$ [$M = \text{Co(II)}$, 1; Cu(II) , 2; Zn(II) , 3]



$\{(\text{Tp}^{\text{Ph}})\text{M}\}$ moiety on the luminescence property of the 1,8-naphthalimide chromophore.^{44–48} The protection of a photosensitizer from solvent in the presence of DNA is known to give a molecular “light-switch” effect that has been observed in ruthenium(II) polypyridyl complexes.^{49,50}

Metal complexes bound to ligands having a 1,8-naphthalimide moiety and 1,8-naphthalimide organic conjugates have been studied for their photoinduced DNA and protein cleavage activity.^{45,48} Gunnlaugsson and co-workers in a recent report have shown that 1,8-naphthalimide conjugates of tris chelates of ruthenium(II) exhibit DNA binding and plasmid DNA cleavage activity in UV-A light.⁴⁵ Herein, we present the synthesis, characterization, DNA and protein binding, and photoinduced DNA and protein cleavage activity of 3d metal complexes $[M(\text{Tp}^{\text{Ph}})(\text{py-nap})](\text{ClO}_4)$, where py-nap is a pyridyl ligand with a 1,8-naphthalimide moiety and $M = \text{Co(II)}$, 1; Cu(II) , 2; and Zn(II) , 3 (Chart 1). We have also prepared $[\text{Cu}(\text{Tp}^{\text{Ph}})(\gamma\text{-pic})](\text{ClO}_4)$ (4) having a nonphotoactive γ -picoline ligand instead of the photoactive py-nap to study the effect of the $\{M(\text{Tp}^{\text{Ph}})\}$ moiety on DNA cleavage and photocytotoxic activity of the complexes. The photocytotoxic property of the Co(II) and Cu(II) complexes has been studied in UV-A light of 365 nm using HeLa cervical cancer cells. We have observed significant photocytotoxicity of the Co(II) complex, while it is nontoxic in the dark. This observation is unprecedented in the PDT chemistry of 1,8-naphthalimide conjugates.

Experimental Section

Materials. The reagents and chemicals were procured from commercial sources and used without further purifications. Standard procedures were used to purify the solvents.⁵¹ Supercoiled (SC) pUC19 DNA (cesium chloride purified) was purchased from Bangalore Genie (India). A tris-(hydroxymethyl)-aminomethane-HCl (Tris-HCl) buffer solution was prepared using deionized and sonicated triple-distilled water. Calf thymus

(CT) DNA, agarose (molecular biology grade), catalase, 1,4-diazabicyclo-[2.2.2]-octan (DABCO), ethidium bromide (EB), bovine serum albumin (BSA), acrylamide, N,N'-methylene-bisacrylamide, ammonium persulphate, N,N,N',N'-tetramethylethylenediamine, 2-mercaptoethanol, tricine, glycerol, sodium dodecyl sulfate (SDS), bromophenol blue, and coomassie brilliant blue R-250 were from Sigma (USA). Literature procedures were followed to prepare the potassium salt of tris(3-phenylpyridyl)borate (KTp^{Ph}) and 2-(4-pyridylmethyl)-2,3-dihydro-1H-benzo[de]isoquinoline-1,3-dione (py-nap).^{52,53}

Methods. Elemental analyses were done using a Thermo Finnigan Flash EA 1112 CHNSO analyzer. The infrared, electronic, and emission spectra were recorded on Perkin-Elmer spectrum one 55, Perkin-Elmer Lambda 35, and Perkin-Elmer LS50B spectrophotometers, respectively. Room temperature magnetic susceptibility data were obtained using a Model 300 Lewis-coil-force magnetometer of George Associates Inc. (Berkeley, USA) make. $\text{Hg}[\text{Co}(\text{NCS})_4]$ was used as a standard. Experimental susceptibility data were corrected for diamagnetic contributions.⁵⁴ Molar conductivity measurements were done using a Control Dynamics (India) conductivity meter. Electro-spray ionization mass spectral measurements were made using a Bruker Daltonics make Esquire 300 Plus ESI model. Cyclic voltammetric measurements were done at 25 °C on an EG&G PAR Model 253 VersaStat potentiostat/galvanostat with electrochemical analysis software 270 using a three-electrode setup consisting of a glassy carbon working, platinum wire auxiliary, and saturated calomel reference electrodes. The electrochemical data were uncorrected for junction potentials.

Preparation of $[M(\text{Tp}^{\text{Ph}})(\text{py-nap})](\text{ClO}_4)$ [$M = \text{Co(II)}$, 1; Cu(II) , 2; Zn(II) , 3]. The complexes were prepared by following a general procedure in which a suspension of KTp^{Ph} (0.1 g, 0.2 mmol) in 10 mL of CH_2Cl_2 was initially stirred for 1 h with a 10 mL CH_2Cl_2 suspension of $[M(\text{H}_2\text{O})_6](\text{ClO}_4)_2$ (0.07 g, 0.2 mmol), followed by an addition of 10 mL of a CH_2Cl_2 solution of py-nap (0.05 g, 0.2 mmol) at 0 °C. The reaction mixture was stirred for 30 min, during which a clear solution was obtained. The solution was filtered, and the product was isolated as a solid on slow evaporation of the solvent. The product was purified by washing with a 1:1 (v/v) mixture of hexane and CH_2Cl_2 and dried in a vacuum over P_4O_{10} . The yield of the complexes was ~60% (0.11 g). Anal. Calcd for $\text{C}_{45}\text{H}_{34}\text{BCoN}_8\text{ClO}_6$ (1): C, 60.87; H, 3.86; N, 12.62. Found: C, 60.66; H, 3.81; N, 12.41. ESI-MS in MeCN: m/z 788.1 $[M - \text{ClO}_4]^+$. Λ_M , $\text{S m}^2 \text{M}^{-1}$ in DMF at 25 °C: 76. FT-IR, cm^{-1} (KBr disk): 3314br, 2926w, 2474m (B–H), 1967s, 1702s, 1661s, 1619m, 1588s, 1491s, 1467s, 1368s, 1237s, 1191s, 1095vs (ClO_4^-), 953m, 846m, 781s, 734m, 696s, 622m, 529w (vs, very strong; s, strong; m, medium; w, weak; br, broad). Electronic spectrum in DMF-Tris-HCl buffer (2:1 v/v) [λ_{max} , nm (ϵ , $\text{M}^{-1} \text{cm}^{-1}$): 530 (20), 354sh (12 100), 341 (14 200) and 259 (41 300) (sh, shoulder). $\mu_{\text{eff}} = 4.47 \mu_B$ at 298 K. Anal. Calcd for $\text{C}_{45}\text{H}_{34}\text{BCuN}_8\text{ClO}_6$ (2): C, 60.55; H, 3.84; N, 12.55. Found: C, 60.38; H, 3.74; N 12.31. ESI-MS in MeCN: m/z 792 $[M - \text{ClO}_4]^+$. Λ_M , $\text{S m}^2 \text{M}^{-1}$ in DMF at 25 °C: 66. FT-IR, cm^{-1} (KBr disk): 3350br, 2926w, 2475m (B–H), 1965s, 1702s, 1662s, 1620m, 1589m, 1491m, 1364m, 1236s, 1193s, 1100vs (ClO_4^-), 954m, 846m, 761s, 696m, 623s, 530w. Electronic spectrum in DMF-Tris-HCl buffer (2:1 v/v) [λ_{max} , nm (ϵ , $\text{M}^{-1} \text{cm}^{-1}$): 669 (50), 338 (10 200), 354sh (8450) and 259 (32 500). $\mu_{\text{eff}} = 1.91 \mu_B$ at 298 K. Anal. Calcd for $\text{C}_{45}\text{H}_{34}\text{BZnN}_8\text{ClO}_6$ (3): C, 60.43; H, 3.83; N, 12.53. Found: C, 60.20; H, 3.63; N, 12.35. ESI-MS in MeCN: m/z 794 $[M - \text{ClO}_4]^+$. Λ_M , $\text{S m}^2 \text{M}^{-1}$ in DMF at 25 °C: 70. FT-IR, cm^{-1} (KBr disk): 3340br, 2916w, 2475m (B–H), 1950s, 1705s, 1675s, 1610m, 1580m, 1475m, 1352m, 1223s, 1191s, 1105vs (ClO_4^-), 950m, 848m, 753s, 691m, 620s, 539w. Electronic spectrum

(44) Cao, H.; Chang, V.; Hernandez, R.; Heagy, M. D. *J. Org. Chem.* **2005**, *70*, 4929.

(45) Ryan, G. J.; Quinn, S.; Gunnlaugsson, T. *Inorg. Chem.* **2008**, *47*, 401.

(46) Saito, I.; Takayama, M.; Sugiyama, H.; Nakatani, K. *J. Am. Chem. Soc.* **1995**, *117*, 6406.

(47) Saito, I.; Takayama, M. *J. Am. Chem. Soc.* **1995**, *117*, 5590.

(48) Abraham, B.; Kelly, L. A. *J. Phys. Chem. B* **2003**, *107*, 12534.

(49) Erkkila, K. E.; Odom, D. T.; Barton, J. K. *Chem. Rev.* **1999**, *99*, 2777.

Hartshorn, R. M.; Barton, J. K. *J. Am. Chem. Soc.* **1992**, *114*, 5919. Friedman, A. E.; Chambron, J. C.; Sauvage, J. P.; Turro, N. J.; Barton, J. K. *J. Am. Chem. Soc.* **1990**, *112*, 4960. Metcalfe, C.; Thomas, J. A. *Chem. Soc. Rev.* **2003**, *32*, 215.

(50) Sun, Y.; Lutterman, D. A.; Turro, C. *Inorg. Chem.* **2008**, *47*, 6427. Arounaguir, S.; Maiya, B. G. *Inorg. Chem.* **1999**, *38*, 842.

(51) Perrin, D. D.; Armarego, W. L. F.; Perrin, D. R. *Purification of Laboratory Chemicals*; Pergamon Press: Oxford, U. K., 1980.

(52) Eichhorn, D. M.; Armstrong, W. H. *Inorg. Chem.* **1990**, *29*, 3607.

(53) Barooah, N.; Tamuly, C.; Baruah, J. J. *Chem. Sci.* **2005**, *117*, 117.

(54) Khan, O. *Molecular Magnetism*; VCH: Weinheim, Germany, 1993.

in DMF-Tris-HCl buffer (2:1 v/v) [λ_{max} , nm (ϵ , $\text{M}^{-1} \text{cm}^{-1}$): 354sh (5950), 340 (7000) and 258 (17300)].

Preparation of [M(Tp^{Ph})(γ -pic)](ClO₄) (4). Complex [Cu(Tp^{Ph})(γ -pic)](ClO₄) (4) was prepared by following the procedure as used for complex 2 in which a suspension of KTp^{Ph} (0.1 g, 0.2 mmol) in 10 mL of CH₂Cl₂ was initially stirred for 1 h with a 10 mL CH₂Cl₂ suspension of [Cu(H₂O)₆](ClO₄)₂ (0.07 g, 0.2 mmol), followed by an addition of 10 mL of a CH₂Cl₂ solution of γ -picoline (0.02 g, 0.2 mmol) at 0 °C. The solid was isolated and purified by washing with the CH₂Cl₂ and hexane and finally dried in a vacuum over P₄O₁₀ (yield: ~60%). Anal. Calcd for C₃₃H₂₉BCuN₇ClO₄ (4): C, 56.83; H, 4.19; N, 14.06. Found: C, 56.63; H, 4.23; N 14.11. ESI-MS in MeCN: m/z 597 [M - ClO₄]⁺. Λ_{M} , S m² M⁻¹ in DMF at 25 °C: 80. FT-IR, cm⁻¹ (KBr disk): 3450br, 2923w, 2469m, 1953w, 1624s, 1450s, 1358m, 1317s, 1261m, 1191s, 1093vs (ClO₄⁻), 963m, 914w, 797m, 757s, 690m, 621w, 493w. Electronic spectrum in DMF-Tris-HCl buffer (2:1 v/v) [λ_{max} , nm (ϵ , $\text{M}^{-1} \text{cm}^{-1}$): 670 (40), 330sh (900) and 259 (26700)].

Solubility and Stability. The complexes were soluble in DMF, DMSO, MeCN, and CH₂Cl₂; sparingly soluble in water; and insoluble in the hydrocarbon solvents. They were stable in the solid and solution phases. Since perchlorate salts of the metal complexes could be potentially explosive, a small quantity of the sample was used with necessary precautions.

DNA Binding Experiments. The interaction of the complexes with CT DNA was studied in Tris-HCl buffer (5 mM Tris-HCl, pH 7.2) containing 1.6–5% DMF at 25 °C. Thermal denaturation studies were done in a melting buffer consisting of 5 mM Na₂HPO₄, 5 mM NaH₂PO₄, 1 mM Na₂EDTA, and 5 mM NaCl. A solution of the CT DNA in the buffer gave a ratio of UV absorbance at 260 and 280 nm of about 1.9:1, indicating that the CT DNA is sufficiently free from protein.⁵⁵ The concentration of CT DNA was measured from its absorption intensity at 260 nm using an ϵ value of 6600 M⁻¹ cm⁻¹.⁵⁶ The concentration of the CT DNA was varied, keeping the complex concentration as constant (50 μM) in absorption titration experiments. Due correction was made for the absorbance of CT DNA itself. Sample equilibration was done for 5 min before recording the spectra. The intrinsic equilibrium binding constant (K_b) values of the complexes to CT DNA were obtained using the McGhee–von Hippel (MvH) method using the expression of Bard and co-workers by monitoring the change in the absorption intensity of the charge-transfer spectral band at 335 nm with an increasing concentration of CT DNA by regression analysis using the equation $(\epsilon_a - \epsilon_f)/(\epsilon_b - \epsilon_f) = (b - (b^2 - 2K_b^2 C_t [\text{DNA}]/s)^{1/2}) / 2K_b C_t$, where $b = 1 + K_b C_t + K_b [\text{DNA}]/2s$, ϵ_a is the extinction coefficient observed for the spectral band at a given DNA concentration, ϵ_f is the extinction coefficient of the complex free in solution, ϵ_b is the extinction coefficient of the complex when fully bound to DNA, K_b is the equilibrium binding constant, C_t is the total complex concentration, $[\text{DNA}]$ is the DNA concentration in nucleotides, and s is the binding site size in base pairs.^{57,58} The nonlinear least-squares analysis was done using Origin Lab, version 7.5. Emission titration was performed by adding CT DNA in 5 mM Tris-HCl (pH 7.2) to a solution of 1–3 (25 μM). The binding constant (K) values were obtained using an equation which is similar to that given above having $(I_a - I_f)/(I_b - I_f)$ instead of $(\epsilon_a - \epsilon_f)/(\epsilon_b - \epsilon_f)$, where I_a is the observed emission intensity of the complex at a given DNA concentration, I_f is the emission intensity of the complex free in solution, and I_b is the emission intensity of the complex when fully bound to DNA when

additional DNA did not change the emission intensity of the complex.⁵⁹

DNA melting experiments were carried out by monitoring the absorption intensity of CT DNA (174 μM) at 260 nm at various temperatures, in both the absence and presence of the metal scorpionates (40 μM). Measurements were carried out using a Perkin-Elmer Lambda 35 spectrophotometer equipped with a Peltier temperature-controlling programmer (PTP 6; ± 0.1 °C) on increasing the temperature of the solution at 0.25 °C per min. Viscometric titrations were performed using a Schott Gerate AVS 310 Automated Viscometer that was thermostatted at 37 ± 0.1 °C in a constant temperature bath. The concentration of CT DNA was 165 μM in NP (nucleotide pairs), and the flow times were measured with an automated timer. Three measurements were taken for each sample to calculate the average flow time. Data were presented as $(\eta/\eta_0)^{1/3}$ versus $[\text{complex}]/[\text{DNA}]$, where η is the viscosity of DNA in the presence of the complex and η_0 that of DNA alone.⁶⁰ Viscosity values were calculated from the observed flowing time of DNA-containing solutions (t) corrected for that of the buffer alone (t_0), $\eta = (t - t_0)/t_0$.

DNA Cleavage Experiments. The chemical nuclease activity of the complexes was studied using SC pUC19 DNA in Tris-HCl/NaCl buffer in the presence of 3-mercaptopropionic acid (MPA) as a reducing agent or hydrogen peroxide (H₂O₂) as an oxidizing agent. Agarose gel electrophoresis was done to determine the extent of cleavage of SC DNA (30 μM , 0.2 μg , 2686 base-pair) by the metal complexes (50 μM) in 50 mM Tris-HCl buffer containing 10% DMF and 50 mM NaCl (pH 7.2). The photoinduced DNA cleavage studies were carried out under illuminated conditions using an UV-A light source at 365 nm (6 W, Bangalore Genie make) and a visible light laser (Spectra Physics Water-Cooled Mixed-Gas Ion Laser Stabilite 2018-RM with beam diameter at $1/e^2$ 1.8 mm \pm 10% and beam divergence with full angle 0.70 mrad \pm 10%). Each sample was incubated for 1.0 h at 37 °C prior to photoexposure with a solution path-length of 5 mm placed at a distance of 10 cm from the light source. The power of the laser beam at the sample position was measured using a Spectra Physics CW Laser Power Meter (model 407A). Following light exposure, each sample was incubated for 1.0 h at 37 °C and analyzed for the photocleaved products using gel electrophoresis. Mechanistic studies were done using different reagents, namely, NaN₃, 200 μM ; DABCO, 200 μM ; DMSO, 4 μL ; catalase, 2 units; and KI, 200 μM . For the D₂O experiment, this solvent was used for dilution of the sample to a volume of 20 μL . The samples after incubation in a dark chamber were added to the loading buffer containing 25% bromophenol blue, 0.25% xylene cyanol, and 30% glycerol (3 μL), and the solution was finally loaded on 1.0% agarose gel containing 1.0 $\mu\text{g}/\text{mL}$ ethidium bromide. Electrophoresis was carried out in a dark room for 2.0 h at 60 V in a Tris-acetate EDTA buffer. UV light was used for visualization of the bands that were photographed. The extent of DNA cleavage was measured from the intensities of the bands using the UVITEC Gel Documentation System. Due corrections were made for the low level of the nicked circular (NC) form present in the original SC DNA sample and for the low affinity of EB binding to SC compared to NC and linear forms of DNA.⁶¹ The concentrations of the complexes and reagents corresponded to the quantity of the sample after dilution to the 20 μL final volume with Tris-HCl buffer. The observed error in measuring the band intensities ranged between 3 and 7%.

Protein Binding and Cleavage Experiments. The protein binding study was performed from tryptophan fluorescence quenching

(55) Merill, C.; Goldman, D.; Sedman, S. A.; Ebert, M. H. *Science* **1980**, *211*, 1437.

(56) Reichman, M. E.; Rice, S. A.; Thomas, C. A.; Doty, P. *J. Am. Chem. Soc.* **1954**, *76*, 3047.

(57) McGhee, J. D.; von Hippel, P. H. *J. Mol. Biol.* **1974**, *86*, 469.

(58) Carter, M. T.; Rodriguez, M.; Bard, A. J. *J. Am. Chem. Soc.* **1989**, *111*, 8901.

(59) Smith, S. R.; Neyhart, G. A.; Kalsbeck, W. A.; Thorp, H. H. *New J. Chem.* **1994**, *18*, 397.

(60) Satyanarayana, S.; Dabrowiak, J. C.; Chaires, J. B. *Biochemistry* **1992**, *31*, 9319.

(61) Bernadou, J.; Pratviel, G.; Bennis, F.; Girardet, M.; Meunier, B. *Biochemistry* **1989**, *28*, 7268.

experiments using BSA (2 μM) as the substrate in phosphate buffer (pH 6.8). Quenching of the emission intensity of tryptophan residues of BSA at 344 nm (excitation wavelength at 295 nm) was monitored using complexes 1–3 in phosphate buffer containing 5% DMF as quenchers with the increasing concentration.⁶² The binding constant (K_{BSA}) values were obtained from a Stern–Volmer plot where I_0/I was plotted against complex concentration: $(I_0/I) = 1 + K_{\text{BSA}} \times [\text{complex}]$, where I_0 and I are the emission intensities of BSA in the absence and presence of the quencher. Photoinduced protein cleavage experiments were done according to the literature procedure described by Kumar and co-workers.⁷ Photochemical protein cleavage studies were done using a freshly prepared solution of BSA (MW: 66 267) in 50 mM Tris-HCl buffer (pH 7.2). The protein solutions (5 μM) containing complexes 1–3 in a Tris-HCl buffer containing 10% DMF having concentrations ranging from 5 to 100 μM were photoirradiated at 365 nm (100 W) for 30 min after 2 h of incubation at 37 °C. Protein samples were evaporated under a vacuum using an EYELA Centrifugal Vaporizer (model CVE-200D). The irradiated samples (50 μL) were dried in a centrifugal vaporizer, and the samples were dissolved in the loading buffer (20 μL) containing SDS (7% w/v), glycerol (4% w/v), Tris-HCl buffer (50 mM, pH 6.8), mercaptoethanol (2% w/v), and bromophenol blue (0.01% w/v). The protein solutions were then denatured on heating to a boil for 3 min. The samples were loaded on a 3% polyacrylamide (stacking) gel.⁶³ Gel electrophoresis was done by applying 60 V until the dye passed into the separating gel from the stacking (3%) gel, and then the voltage was increased to 120 V. The gels were run for 1.5 h, followed by staining with a Coomassie Brilliant Blue R-250 solution (acetic acid/methanol/water 1:2:7 v/v), and destaining was done with a water/methanol/acetic acid mixture (5:4:1 v/v) for 4 h. The gels were scanned with a HP Scanjet G3010 scanner, and the images were processed using Adobe Photoshop. Molecular weight markers were used in each gel to calibrate the molecular weights of the BSA. The presence of reactive oxygen species was investigated by carrying out the photoinduced protein cleavage experiment in the presence of various additives like DABCO (3 mM), NaN_3 (3 mM), KI (3 mM), and DMSO (20 μL).

Cell Culture and Photocytotoxicity Experiments. The photocytotoxicity of complexes 1, 2, and 4 and the ligands py-nap and KTp^{Ph} was determined using a (3-(4,5-dimethylthiazol-2-yl)-2,5-diphenyltetrazolium bromide (MTT) assay, which is based on the ability of mitochondrial dehydrogenases of viable cells to cleave the tetrazolium rings of MTT forming dark purple membrane-impermeable crystals of formazan that can be quantified at 595 nm on solubilization in DMSO.⁶⁴ Human cervical carcinoma HeLa cells (~8000) were plated in a 96-well culture plate in DMEM containing 10% FBS, and after 24 h of incubation at 37 °C in a CO_2 incubator, various concentrations of complexes dissolved in 1% DMSO were added to the cells and incubation was continued for 3 h in the dark. After the incubation period, the medium was replaced with fresh PBS and photoexposed to UV-A light (365 nm, 0.549 J cm^{-2}) from a 6 W UV-A lamp (UVITEC make). After photoexposure, PBS was removed and replaced with DMEM/10% FBS, and incubation was continued for a further 24 h in the dark. Thereafter, 20 μL of 5 mg mL^{-1} of MTT was added to each well and incubated for an additional 3 h. The culture medium was replaced with 200 μL of DMSO to dissolve the formazan crystals formed, and absorbance at 595 nm was determined with a BIORAD ELISA plate reader. Cytotoxicity of the complexes was measured as the percentage ratio of the absorbance of the treated cells to the untreated controls. The IC_{50} values were determined by nonlinear regression analysis (GraphPad Prism 5.0).

Table 1. Selected Physicochemical Data for the Complexes $[\text{M}(\text{Tp}^{\text{Ph}})(\text{py-nap})](\text{ClO}_4)$ [$\text{M} = \text{Co}(\text{II}), 1; \text{Cu}(\text{II}), 2; \text{Zn}(\text{II}), 3$]

	1	2	3
IR, ^a cm^{-1} : $\nu(\text{B-H})$	2474	2475	2475
$\nu(\text{C=O})$	1702, 1661	1702, 1662	1705, 1675
$\nu(\text{ClO}_4^-)$	1095	1100	1105
λ , nm (ϵ , $\text{M}^{-1} \text{cm}^{-1}$) ^b	531(20)	669 (50)	
μ_{eff}^c	4.47	1.91	
λ_f , nm (Φ_f) ^d	388 (0.012)	389 (0.015)	389 (0.020)
Λ_m , ^e $\text{S m}^2 \text{M}^{-1}$	76	66	70

^a In the KBr phase. ^b Visible electronic spectral band in DMF-Tris buffer (2:1 v/v). ^c μ_{eff} in μ_{B} for solid powdered samples at 298 K. ^d Emission spectral band in DMF-Tris buffer (2:1 v/v). Quantum yield (Φ_f) for py-nap is 0.018. ^e Molar conductance in DMF.

Results and Discussion

Synthesis and General Aspects. The bivalent 3d-metal ternary complexes of formulation $[\text{M}(\text{Tp}^{\text{Ph}})(\text{py-nap})](\text{ClO}_4)$ [$\text{M} = \text{Co}(\text{II}), 1; \text{Cu}(\text{II}), 2; \text{Zn}(\text{II}), 3$] and $[\text{M}(\text{Tp}^{\text{Ph}})(\gamma\text{-pic})](\text{ClO}_4)$ (4) have been synthesized in high yield from the reaction of $[\text{M}(\text{H}_2\text{O})_6](\text{ClO}_4)_2$ with the potassium salt of tris(3-phenylpyrazolyl)borate (KTp^{Ph}) and py-nap or γ -picoline and isolated as perchlorate salts (Chart 1). The complexes have been characterized from the analytical and mass spectral data. Selected physicochemical data for complexes 1–3 are given in Table 1. The complexes are stable in the solution phase, as evidenced from the mass spectral features showing only the molecular ion peaks (Figures S1–S4, Supporting Information). The 1:1 electrolytic py-nap complexes show characteristic IR stretching bands for ClO_4^- , B–H (Tp^{Ph}), and C=O (py-nap) at ~ 1090 , ~ 2500 , and $\sim 1700 \text{ cm}^{-1}$, respectively.^{41–43,53} The Co(II) and Cu(II) complexes display a visible spectral band in an aqueous DMF (1:2 v/v) medium (Figure 1). The ligand-centered electronic spectral bands have been observed in the UV range. Complexes 1–3 exhibit an emission spectral peak at ~ 385 nm in aqueous DMF (1:2 v/v) on excitation at their absorption maximum near 350 nm (Figure S5 in Supporting Information). The quantum yield (ϕ) values of 1–3 are 0.012, 0.015, and 0.020, respectively. The quantum yield value of the py-nap ligand alone is 0.018.⁶⁵ The Co(II) and Cu(II) complexes are three- and one-electron paramagnetic, while the Zn(II) complex is diamagnetic. The complexes do not show any metal-based redox process in DMF/0.1 M TBAP. A ligand-centered redox process has been observed at -1.120 V (Figure S6 in Supporting Information).

DNA Binding Experiments. The binding propensity of the ternary 3d-metal scorpionates 1–3 to CT DNA has been studied using various techniques. The DNA binding data are given in Table 2. Electronic spectral titrations have been done to determine the intrinsic equilibrium binding constant (K_b) and the binding site size(s) of the complexes by monitoring the change in the absorption intensity of the ligand-centered bands (Figure S7 in Supporting Information). Intercalative binding of a complex to DNA base pairs generally gives hypochromism and a red shift (bathochromism) of the absorption band.⁶⁶ The extent of hypochromism indicates the

(62) Hu, Y.-J.; Liu, Y.; Wang, J.-B.; Xiaob, X.-H.; Qu, S. S. *J. Pharm. Biomed. Anal.* **2004**, *36*, 915.

(63) Schägger, H.; von Jagow, G. *Anal. Biochem.* **1987**, *166*, 368.

(64) Mosmann, T. *J. Immunol. Methods* **1983**, *65*, 55.

(65) Cao, T.; Webber, S. E. *Macromolecules* **1991**, *24*, 79.

(66) Bilakhiya, A. K.; Tyagi, B.; Paul, P.; Natarajan, P. *Inorg. Chem.* **2002**, *41*, 3830. Tysoe, S. A.; Morgan, R. J.; Baker, A. D.; Strekas, T. C. *J. Phys. Chem.* **1993**, *97*, 1707.

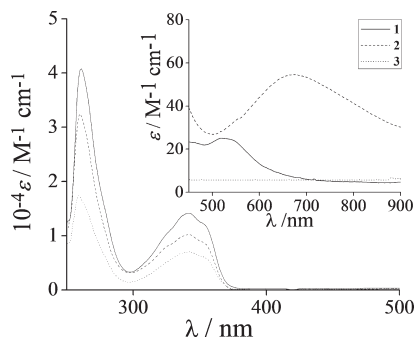


Figure 1. Electronic spectra of [Co(Tp^{Ph})(py-nap)](ClO₄) (**1**) (—), [Cu(Tp^{Ph})(py-nap)](ClO₄) (**2**) (---), and [Zn(Tp^{Ph})(py-nap)](ClO₄) (**3**) (···) in DMF-Tris-HCl buffer (2:1 v/v).

Table 2. DNA and BSA Binding Data for the Complexes [M(Tp^{Ph})(py-nap)](ClO₄) [M = Co(II), **1**; Cu(II), **2**; Zn(II), **3**]

	1	2	3
$10^{-5}K_b,^a M^{-1}$ [s, b.p.]	9.0 ± 0.2 [0.1]	8.1 ± 0.4 [0.3]	8.2 ± 0.1 [0.2]
$10^{-6}K_b,^b M^{-1}$	5.6 ± 0.2	3.6 ± 0.2	4.6 ± 0.1
$\Delta T_m,^c \text{ }^\circ\text{C}$	3.5	3.4	3.1
$10^{-3}K_{BSA},^d M^{-1}$	1.8	1.1	1.6

^a Intrinsic DNA binding constant (s, binding site size). ^b DNA binding constant by emission spectral method. ^c Change in DNA melting temperature. ^d BSA (bovine serum albumin) binding constant from fluorescence spectral measurements.

strength of an intercalative binding. The present complexes show 30–40% hypochromism upon binding to CT DNA. The binding constant values of $\sim 10^5 M^{-1}$ suggest good DNA binding propensity of the py-nap complexes, possibly due to the presence of the 1,8-naphthalimide moiety. We have also investigated the DNA “light-switch” effect of the complexes and obtained the DNA binding constant values using the emission property of these complexes. The complexes in aqueous DMF display emission at ~ 385 nm. The emission intensity of a $25 \mu M$ metal complex has been found to increase significantly ($I/I_0 = 1.58$ to 1.65) on the addition of CT DNA in Tris buffer. The emission intensity gets saturated, finally showing a red shift of 6–10 nm in the emission maxima (Figure S8 in Supporting Information). The observed enhancement of the emission intensity of the complexes on binding to CT DNA is akin to the molecular “light-switch” effect known for ruthenium polypyridyl complexes having a DNA intercalating dipyrrophenazine ligand.⁴⁹ The planar naphthalimide moiety in the py-nap complexes could bind to DNA intercalatively, resulting in an enhancement in the emission intensity. The binding constant values obtained from the emission binding experiment are $\sim 10^6 M^{-1}$ (Table 2).

We have also done DNA thermal denaturation and viscosity measurements to get further insights into the DNA binding nature of the complexes. In a thermal denaturation study, an increase in the solution temperature causes a gradual dissociation of the double-strand (ds) DNA to single strands. We have observed a significant increase of 3–4 $^\circ\text{C}$ in the CT DNA melting temperature in the presence of complexes **1–3** (Figure 2). The ΔT_m values suggest a possible intercalative binding

nature of the complexes.⁶⁷ The ΔT_m values reported for analogous 3d-metal scorpionates [M(Tp^{Ph})(dpq)](ClO₄), where dpq is dipyrroquinoxaline, are ~ 2 $^\circ\text{C}$.⁴³ It appears that py-nap with a 1,8-naphthalimide moiety is a better DNA intercalator than the dpq ligand. Viscosity measurements have been done using solutions of CT DNA incubated with the complexes to determine the relative specific viscosity (η/η_0) of CT DNA. Since η/η_0 of DNA gives a measure of the increase in the contour length associated with the separation of DNA base pairs caused by an intercalating ligand, a classical DNA intercalator like EB shows a significant increase in the viscosity of the DNA solutions, where η and η_0 are the specific viscosities of DNA in the presence and absence of the complexes, respectively. In contrast, a partial or nonintercalating ligand could result in a less pronounced effect on the viscosity.⁶⁸ The relative viscosity of DNA is found to increase significantly on increasing the concentration of **1–3**. The plot of relative specific viscosity (η/η_0)^{1/3} versus the [complex]/[DNA] ratio for **1–3** shows a significant change in the viscosity (Figure 2). The contour length and relative viscosity of DNA follows the equation (η/η_0) = $(L/L_0)^{1/3}$, where L and L_0 are the contour length of DNA in the presence and absence of the complexes, respectively.⁶⁹ Viscosity results suggest primarily a DNA intercalative binding nature of the complexes. In summary, the binding data indicate a partial intercalative mode of binding of the complexes to CT DNA.

Chemical Nuclease Activity. The redox active transition metal complexes could show good chemical nuclease activity.⁶ For example, redox-active binary copper(II) complexes of phenanthroline bases with a quasi-reversible Cu(II)/Cu(I) couple are known to show efficient chemical nuclease activity in the presence of a reducing agent.⁷⁰ The redox-inactive complexes **1–3** do not show any significant chemical nuclease activity in the presence of 3-mercaptopyruvic acid as a reducing agent or hydrogen peroxide as an oxidizing agent (Figure S9 in Supporting Information). A $50 \mu M$ solution of the copper(II) complex **2** shows $\sim 10\%$ cleavage of SC DNA ($30 \mu M$) in the presence of MPA ($500 \mu M$). The Co(II) complex **1** ($50 \mu M$) cleaves only 12% of SC DNA on treatment with H₂O₂ ($500 \mu M$). Earlier reports have shown that scorpionates of formulation [M(Tp^{Ph})(B)], where B is a phenanthroline base and M is a bivalent 3d metal ion, exhibit only moderate chemical nuclease activity in comparison to bis-phen copper(II) species that are known to be excellent chemical nucleases.^{41–43,70}

DNA Photocleavage Activity. The photoinduced DNA cleavage activity of the complexes has been studied using SC pUC19 DNA ($30 \mu M$, $0.2 \mu g$) in a Tris-HCl/NaCl buffer on irradiation with monochromatic UV-A light of 365 nm (6 W) and visible light of a tunable Ar–Kr laser. Selected photoinduced DNA cleavage data are given in Table 3. It has been observed that [Co(Tp^{Ph})(py-nap)](ClO₄) (**1**) and [Cu(Tp^{Ph})(py-nap)](ClO₄) (**2**) are efficient photocleavers of SC DNA in UV-A light (Figure 3, Figure S10 in Supporting Information). Complex

(68) Gabbay, E. J.; Scofield, R. E.; Baxter, C. S. *J. Am. Chem. Soc.* **1973**, *95*, 7850. Veal, J. M.; Rill, R. L. *Biochemistry* **1991**, *30*, 1132.

(69) Cohen, G.; Eisenberg, H. *Biopolymers* **1969**, *8*, 45.

(70) Sigman, D. S. *Acc. Chem. Res.* **1986**, *19*, 180.

(67) Vaidyanathan, G. V.; Nair, B. U. *J. Inorg. Biochem.* **2003**, *95*, 334.

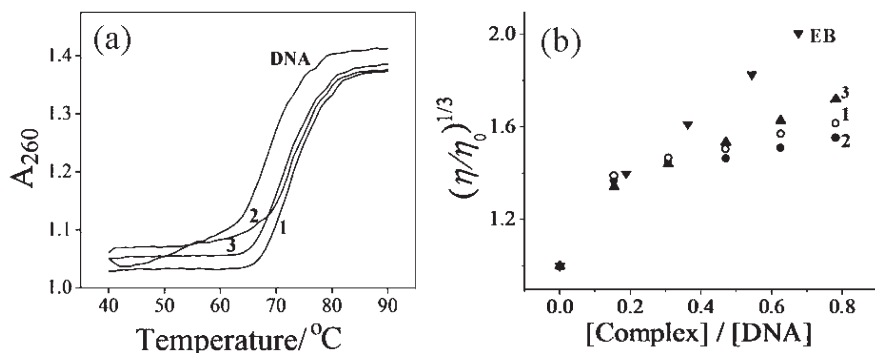


Figure 2. (a) DNA melting plots for CT-DNA (174 μM) in the absence and presence of complexes 1–3. (b) Effect of addition of increasing amount of the complexes [1 (○), 2 (●) and 3 (▲)] on relative viscosity of CT DNA (165 μM) at 37.0 (± 0.1) $^{\circ}\text{C}$ in 5 mM Tris-HCl buffer (pH = 7.2).

Table 3. Selected SC pUC19 DNA (0.2 μg , 30 μM) Cleavage Data of the Complexes $[\text{M}(\text{Tp}^{\text{Ph}})(\text{py-nap})](\text{ClO}_4)$ [M = Co(II), 1; Cu(II), 2; Zn(II), 3] on Irradiation with UV-A and Visible Light

reaction condition	λ , nm ^a	%NC ^b
DNA Control	365	3
DNA + py-nap(50 μM)	365	15
DNA + 1 (50 μM)	365	85
DNA + 1 (150 μM)	514	15
DNA + 2 (50 μM)	365	90
DNA + 2 (150 μM)	647.1	45
DNA + 2 (150 μM)	676	55
DNA + 2 (150 μM)	> 750	60
DNA + 3 (50 μM)	365	50

^a Photoexposure time (t) = 2 h. ^b NC is nicked circular form of SC DNA.

$[\text{Zn}(\text{Tp}^{\text{Ph}})(\text{py-nap})](\text{ClO}_4)$ (**3**) shows only moderate DNA photocleavage activity. A 50 μM solution of the Co(II) and Cu(II) complexes cleaves $\sim 85\%$ of SC DNA to its NC form at 365 nm on 2 h of photoexposure (Figure 3, lanes 6 and 7). The Zn(II) complex (**3**) cleaves $\sim 50\%$ of SC DNA (Figure 3, lane 8). The py-nap ligand alone does not show any significant photocleavage of DNA under similar reaction conditions. The complexes do not cleave SC DNA in the dark, thus excluding the possibility of any hydrolytic cleavage of SC DNA. The 1,8-naphthalimide chromophore of py-nap in the metal-bound form seems to act as a photosensitizer to generate the photoexcited state at 365 nm.⁴⁵

The DNA cleavage activity of the complexes has also been studied in visible light. The Cu(II) complex (**2**) cleaves DNA in red light (Figure 4, Figure S11 in Supporting Information). A 150 μM solution of **2** on irradiation at 647.1 nm (100 mW) or 676 nm (30 mW) for 2 h exhibits $\sim 45\%$ and $\sim 55\%$ cleavage of SC DNA, respectively (Figure 4, lanes 6 and 7). The Cu(II) complex shows moderate DNA photocleavage activity at near-IR wavelength of > 750 nm ($\sim 60\%$ cleavage). The Co(II) complex is a relatively poor cleaver of DNA in visible light of 514 nm. This could possibly be due to low molar extinction coefficient value of the visible electronic band of **1** thus making any metal-assisted photosensitization process unfavorable. The d^{10} -Zn(II) complex (**3**) is cleavage inactive in visible light in absence of any electronic band in the visible region.

To ascertain the stability of the ternary structures in the reaction medium, we have carried out photoinduced DNA cleavage experiments in red light of 647.1 nm using

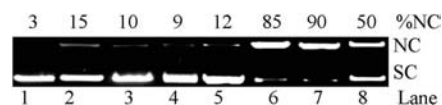


Figure 3. Cleavage of SC pUC19 DNA (0.2 μg , 30 μM) by complexes 1–3 (50 μM) in 50 mM Tris-HCl/NaCl buffer (pH, 7.2) containing 10% DMF on photoirradiation at 365 nm (6 W) with a photoexposure time of 2 h for lanes 1, 2, 6–8. Lane 1, DNA control; lane 2, DNA + py-nap (50 μM); lanes 3–5, DNA + 1–3 (in dark); lanes 6–8, DNA + 1–3.

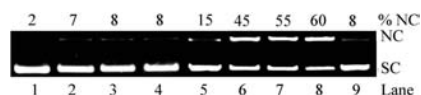


Figure 4. Cleavage of SC pUC19 DNA (0.2 μg , 30 μM) by complexes 1–3 (150 μM) in visible light of 514 nm (100 mW), 647.1 nm (100 mW), 676 nm (30 mW), and > 750 nm (30 mW) for an exposure time of 2 h for lanes 1, 5–9. Lane 1, DNA control (647.1 nm); lanes 2–4, DNA + 1–3 (in dark); lane 5, DNA + 1 (514 nm); lane 6, DNA + 2 (647.1 nm); lane 7, DNA + 2 (676 nm); lane 8, DNA + 2 (> 750 nm); lane 9, DNA + 3 (647.1 nm).

complex $[\text{Cu}(\text{Tp}^{\text{Ph}})(\gamma\text{-pic})](\text{ClO}_4)$ (**4**) as a control, the py-nap ligand alone, and a 1:1 mixture of both py-nap and complex **4** (Figure S11 in Supporting Information). It has been observed that py-nap (150 μM) alone or a mixture of py-nap and $[\text{Cu}(\text{Tp}^{\text{Ph}})(\gamma\text{-pic})](\text{ClO}_4)$ (**4**; 150 μM in 1:1 molar ratio) shows dark toxicity of $\sim 20\%$. Complex **4** or $[\text{Cu}(\text{Tp}^{\text{Ph}})(\text{py-nap})](\text{ClO}_4)$ (**2**) exhibits less dark toxicity ($\sim 5\%$ DNA cleavage), indicating no loss of the pyridyl ligand from the ternary structure of $[\text{Cu}(\text{Tp}^{\text{Ph}})(\gamma\text{-pic})](\text{ClO}_4)$ (**4**) and $[\text{Cu}(\text{Tp}^{\text{Ph}})(\text{py-nap})](\text{ClO}_4)$ (**2**) in the reaction medium. A 150 μM py-nap ligand alone shows $\sim 22\%$ cleavage of SC DNA in red light of 647.1 nm. This value is very much similar to the dark toxicity of the ligand. The control species **4** displays $\sim 8\%$ cleavage at this concentration at 647.1 nm. The poor cleavage activity of **4** could be due to the absence of any photosensitizer in the complex. The mixture of py-nap ligand and $[\text{Cu}(\text{Tp}^{\text{Ph}})(\gamma\text{-pic})](\text{ClO}_4)$ (**4**) shows only 23% DNA cleavage, and again this value is very similar to the dark toxicity of the py-nap ligand. Interestingly, complex $[\text{Cu}(\text{Tp}^{\text{Ph}})(\text{py-nap})](\text{ClO}_4)$ (**2**) shows $\sim 45\%$ DNA cleavage in red light. Any loss of py-nap from the complex should reduce the cleavage activity of the resulting species due to a loss of the photoactive ligand, and a complete loss of py-nap from the structure should give $\sim 23\%$ DNA cleavage. The photoinduced DNA cleavage data in complexes **2** and **4** along with that of the py-nap ligand indicate the stability of the ternary structures in the reaction medium.

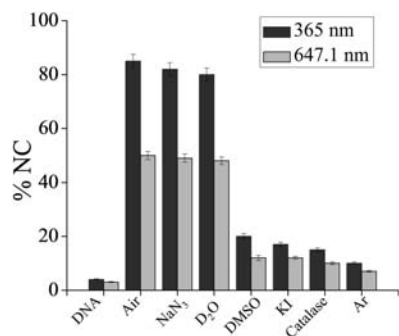


Figure 5. Bar diagram showing the extent of photocleavage of SC pUC19 DNA (0.2 μg , 30 μM) by complex **2** at 365 nm (50 μM) and >750 nm (150 μM) in the presence of different additives for 2 h of exposure time in 50 mM Tris-HCl/NaCl buffer (pH = 7.2).

The DNA cleavage activity of the complexes has been studied in the presence of several additives to understand the mechanistic pathway involved in the DNA photocleavage reaction (Figure 5). The complexes do not show any photocleavage of DNA under an argon atmosphere indicating the necessity of oxygen to produce reactive oxygen species. The complexes show significant inhibition of DNA cleavage in the presence of hydroxyl radical scavengers like DMSO, KI, and catalase, suggesting the possible involvement of hydroxyl radicals as the reactive species. The singlet oxygen quenchers like NaN_3 and DABCO do not inhibit the cleavage activity, and there has been no enhancement in the DNA cleavage activity in D_2O , indicating the non-involvement of a type-II pathway.⁷¹

Protein Binding and Photoinduced Protein Cleavage. An emission quenching experiment has been used to determine the binding constant of the complexes to BSA. The emission of BSA occurs due to the presence of the tryptophan residues, namely, trp-134 and trp-21. The intensity of the emission depends on the exposure of the tryptophan residues to the nearby polar environment and to the quenching groups like protonated carbonyl, protonated imidazole, and tyrosinate anions through molecular interaction.⁷² We have observed that the emission intensity gets quenched gradually on increasing the complex concentration, possibly due to changes in the secondary/tertiary structure of BSA in phosphate buffer, affecting the orientation of the tryptophan residues of BSA (Figure S12 in Supporting Information). The addition of the complex to BSA increases the emission intensity at ~ 380 nm (excitation at 340 nm). This could be due to a molecular “light-switch” effect in which the extent of solvent quenching on the emission intensity of the complexes is reduced due to partial intercalative binding of the complexes to the hydrophobic part of BSA. The K_{BSA} values of the complexes are $\sim 10^5 \text{ M}^{-1}$ (Table 2).

The dose-dependent photoinduced model protease activity of complexes **1–3** against 5 μM BSA in a Tris-HCl buffer medium has been studied by SDS-PAGE (Figure 6). The untreated BSA band is compared to determine the extent of photoinduced protein cleavage. Complexes **1** and **2** have been found to be active in cleaving BSA in a nonspecific manner on photoexposure

to UV-A light (100 W) of 365 nm. We have observed fading or smearing of the BSA band on varying the complex concentration from 5 to 100 μM for an exposure time of 30 min. The Zn(II) complex **3** does not show any cleavage activity. The complexes do not show any protein cleavage activity in the dark, thus ruling out any hydrolytic protein damage. No significant protein cleavage activity is observed in visible light. The involvement of reactive oxygen species in the cleavage reaction has been investigated by carrying out the photoinduced protein cleavage experiments in the presence of singlet oxygen quenchers, namely, DABCO (3 mM) and NaN_3 (3 mM), and hydroxyl radical scavengers, namely, KI (3 mM) and DMSO (20 μL). The complexes do not show any inhibition in the BSA cleavage activity in the presence of NaN_3 and DABCO. KI and DMSO show significant reduction in the BSA cleavage activity, suggesting the involvement of hydroxyl radicals as the reactive species (Figure S13 in Supporting Information).

Photocytotoxicity in HeLa Cells. The photocytotoxic behavior of the Co(II) and Cu(II) complexes has been studied using the human cervical cell line (HeLa) using the MTT assay under UV-A light (365 nm, 0.549 J cm^{-2} ; Figure S14 in the Supporting Information). The live cells reduce the yellow tetrazole to insoluble purple crystals of formazan that, upon solubilization in DMSO, can be quantified at 595 nm to measure the cell viability. The Co(II) complex upon incubation for 4 h in the dark followed by photoexposure to UV-A light and recovery for 24 h has shown a dose-dependent reduction in cell viability, giving an IC_{50} value of 32 μM . In comparison, the cells that have been unexposed to the UV-A light do not exhibit any reduction in cell viability as compared to the untreated controls. This is in contrast to mononaphthalimides and bis-naphthalimides which exhibit significantly high cytotoxicity in the dark.⁷³ The absence of any aromatic substituent and the presence of metal coordination to py-nap thus have a large impact on the dark toxicity of the complex, proving the biocompatibility of the metal and the ligand system constituting the complex. The Cu(II) complex, on the other hand, shows significantly high dark toxicity (IC_{50} value of 29.7 μM), perhaps due to the intracellular redox processes that could generate cytotoxic OH^\bullet radicals by the reduction of Cu(II) to Cu(I). Moreover, this redox cycling of the metal oxidation state has a large effect on the photocytotoxic potential of the Cu(II) complex, giving an IC_{50} value of 18.6 μM in UV-A light.

We have carried out further cellular experiments to determine that the observed cellular activity is due to the ternary complexes and not to any cumulative effect arising from two different fragments resulting from the degradation of the ternary structures in a cellular medium. We have used complex $[\text{Cu}(\text{Tp}^{\text{Ph}})(\gamma\text{-pic})](\text{ClO}_4)$ (**4**) as a control and the py-nap ligand (Figure S15 in Supporting Information). The DNA-intercalator photoactive py-nap alone gives IC_{50} values of 124.8 and 41.42 μM in the dark and in UV-A light of 365 nm, respectively. The IC_{50} values for $[\text{Cu}(\text{Tp}^{\text{Ph}})(\text{py-nap})](\text{ClO}_4)$ (**2**) are 29.7 and

(71) Khan, A. U. *J. Phys. Chem.* **1976**, *80*, 2219.

(72) Peters, T. *Adv. Protein Chem.* **1985**, *37*, 161.

(73) Bousquest, P. F.; Braña, M. F.; Conlon, D.; Fitzgerald, K. M.; Perron, D.; Cocchiario, C.; Miller, R.; Moran, M.; George, J.; Qian, X.-D.; Keilhauer, G.; Romerdahl, C. A. *Cancer Res.* **1995**, *55*, 1176.

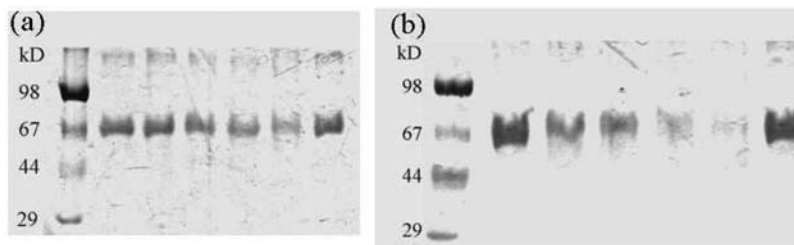


Figure 6. SDS-PAGE diagram showing photocleavage of bovine serum albumin (BSA, 5 μM) in UV-A light of 365 nm (100 W) by complexes $[\text{M}(\text{Tp}^{\text{Ph}})(\text{py-nap})](\text{ClO}_4)$ ($\text{M} = \text{Co}$, **1**; Cu , **2**) in 50 mM Tris-HCl buffer having 10% DMF (pH = 7.2) for an exposure time of 2 h. Panels a and b are for complexes **1** and **2**, respectively: lane 1, molecular marker; lane 2, BSA control; lane 3, BSA + complex (5 μM); lane 4, BSA + complex (25 μM); lane 5, BSA + complex (50 μM); lane 6, BSA + complex (100 μM); lane 7, BSA + complex (100 μM , in dark).

18.6 μM in the dark and light, respectively, under the same reaction conditions. Control complex $[\text{Cu}(\text{Tp}^{\text{Ph}})(\gamma\text{-pic})](\text{ClO}_4)$ gives a similar IC_{50} value to that of complex **2** in the dark. Complex **2** shows an enhancement in cellular activity in the light. A comparison of the cellular data of **2**, **4**, and py-nap indicates the stability of the ternary structures in the cellular medium. The photocytotoxic behavior of the Co(II) complex of py-nap is less than that of the reported Fe(III) and V(IV) complexes of the dipyrrophenazine (dppz) ligand, but suitable ligand design could enhance the photocytotoxic behavior of the Co(II) complexes.^{37,38}

Conclusions

We present here the chemistry of 3d-metal scorpionates having a pyridyl ligand with a 1,8-naphthalimide chromophore showing DNA and BSA protein binding propensities. The effective enclosure of the chromophore in the $\{\text{M}(\text{Tp}^{\text{Ph}})\}$ molecular bowl has resulted in poor chemical nuclease but significant photoinduced DNA cleavage activity of the complexes in UV-A light. The Cu(II) complex shows DNA cleavage activity at a near-IR wavelength of > 750 nm. The complexes show a molecular “light-switch” effect in the presence of CT DNA or BSA. The Co(II) and Cu(II) complexes display photoinduced BSA cleavage activity at 365 nm. Mechanistic investigations reveal the involvement of

hydroxyl radicals in photoinduced DNA and BSA cleavage reactions. The Co(II) complex exhibits significant photocytotoxicity in HeLa cancer cells in UV-A light. The results are of significance toward designing and developing the hitherto unknown chemistry of metal scorpionates for cellular applications in PDT and as antimetastasis agents.

Acknowledgment. We thank the Department of Science and Technology, Government of India, for financial support (SR/S5/MBD-02/2007). We also thank the Council of Scientific and Industrial Research, New Delhi, for research fellowships to S.R. and S.S. We are grateful to the Alexander von Humboldt Foundation, Germany, for an electrochemical system. A.R.C. thanks DST for a J. C. Bose national fellowship.

Supporting Information Available: ESI-MS (Figures S1–S4), emission spectra (Figure S5), cyclic voltammograms (Figure S6), DNA binding plot from absorption spectral titration (Figure S7) and fluorescence spectral titration (Figure S8), chemical nuclease activity (Figure S9), photoinduced DNA cleavage activity at 365 nm (Figure S10) and in visible light (Figure S11), fluorescence binding plots of BSA (Figure S12), mechanistic data on protein cleavage (Figure S13), and cytotoxicity plots for the complexes (Figure S14) and for the control species (Figure S15). This material is available free of charge via the Internet at <http://pubs.acs.org>.